Carbon-13 chemical shift tensor correlation via spin diffusion in solid tropolone using switched-angle spinning spectroscopy

R. G. Larsen, Y. K. Lee, B. He, and J. O. Yang
Material Science Division, Lawrence Berkeley Laboratory and Department of Chemistry, University of California, Berkeley, California 94720

Z. Luz
Chemical Physics Department, Weizmann Institute of Science, 76100 Rehovot, Israel

H. Zimmermann
Max-Planck-Institut für Medizinische Forschung, AG Molekülkristalle, Jahnstrasse 29, 69120 Heidelberg, Germany

A. Pines
Material Science Division, Lawrence Berkeley Laboratory and Department of Chemistry, University of California, Berkeley, California 94720

(Received 25 May 1995; accepted 29 August 1995)

In switched-angle spinning spectroscopy (SAS) a sample is spun about different angles, β, relative to the magnetic field, during various periods of the experiment. In the present work, SAS is combined with two-dimensional exchange spectroscopy in order to correlate carbon-13 chemical shift tensors of the carbonyl (1) and hydroxyl (2) carbons of tropolone. Experiments were performed on a sample enriched to 25 at. % in each of these sites (at different molecules). At this level of enrichment the dominant exchange mechanism between the two sites involves spin diffusion. The experiment consists of a preparation period during which the sample spins at the magic angle and the magnetization of one of the sites is quenched by means of a selective pulse sequence. During the rest of the experiment the sample spins with its axis away from the magic angle except for a short period just before the detection where the axis is switched to the magic angle in order to select the magnetization to be detected. Experiments were performed for all four possible combinations of the initial and final magnetizations, thus providing chemical shift correlations between carbons 1,1′, 2, and 2′ in the two magnetically inequivalent (but symmetry related) molecules in the unit cell. Combining these results with the known crystal structure of tropolone (neglecting a small tilt between the perpendicular to the molecular plane and the crystallographic **c**-axis) provides information on the orientation and magnitude of the chemical shift tensors of the two types of carbons. The principal values (in ppm) are $\sigma^1_{xx}=65$, $\sigma^1_{yy}=33$, $\sigma^1_{zz}=-98$, $\sigma^2_{xx}=77$, $\sigma^2_{yy}=17$, and $\sigma^2_{zz}=-94$. Assuming σ_{zz} to be perpendicular to the molecular plane, the orientations of the σ_{yy}'s are 12° off the $C^1=0$ bond (toward the hydroxyl carbon) for carbon 1 and 10° off the $C^3=C^2$ bond (away from the carbonyl carbon) for carbon 2. © *1995 American Institute of Physics.*

I. INTRODUCTION

Two-dimensional nuclear magnetic resonance (2D NMR) exchange experiments have provided a wealth of information on molecular self-diffusion and spin diffusion in solids.[1] The results of such experiments are displayed in terms of 2D contour plots of the conditional probability, $S(\omega_1,\omega_2;\tau_m)$, that a spin having the initial precession frequency ω_1 will, due to some spin exchange process, resonate at a frequency ω_2 at a time τ_m, called the mixing time, later. Most of the reported experiments involved compounds with a single type of NMR active nuclei as, for example, in specifically deuterated materials, or in compounds with a single type of carbon. When the system contains two or more different types of NMR active nuclei, overlap between their signals can blur the 2D correlation diagram and make quantitative analysis difficult. Several methods have been designed to overcome this difficulty. In one approach,[2,3] 2D exchange spectra are recorded under conditions of magic angle spinning (MAS) at a low-spinning frequency, ω_r, ($\omega_r<\omega_0\delta\sigma$) and with a mixing time synchronized with the rotation period. Under these conditions separate sets of spinning sidebands are observed for different types of nuclei and the spin exchange is manifested by cross peaks linking corresponding sidebands.

Another approach involves an extension of 2D variable angle correlation spectroscopy [2D-VACSY, see Fig. 1(a)].[4] In this experiment, spectra of a rapidly spinning sample ($\omega_r>\omega_0\delta\sigma$) are recorded for different inclinations, β, of the spinner axis with respect to the external magnetic field. Interpolation, followed by two-dimensional Fourier transformation of the resulting data, yields separate anisotropic powder patterns along one dimension, according to the isotropic chemical shifts of the various nuclei in the second dimension. Extension of the method to exchange spectroscopy requires another time variable in order to correlate the interchanging magnetic shielding tensors. Two versions of such (3D) experiments are depicted in Figs. 1(b) and 1(c).[5,6] In the 3D-VACSY-S-exchange version the evolution period, t_1 is fixed and the spinning axis is switched during the mixing time from β_1 at t_1 to β_2 at the detection period t_2. In the 3D-VACSY-T-exchange version, β is the same during evolution and detection, but t_1 is incremented, as in the usual 2D

 0021-9606/95/103(22)/9844/11/$6.00

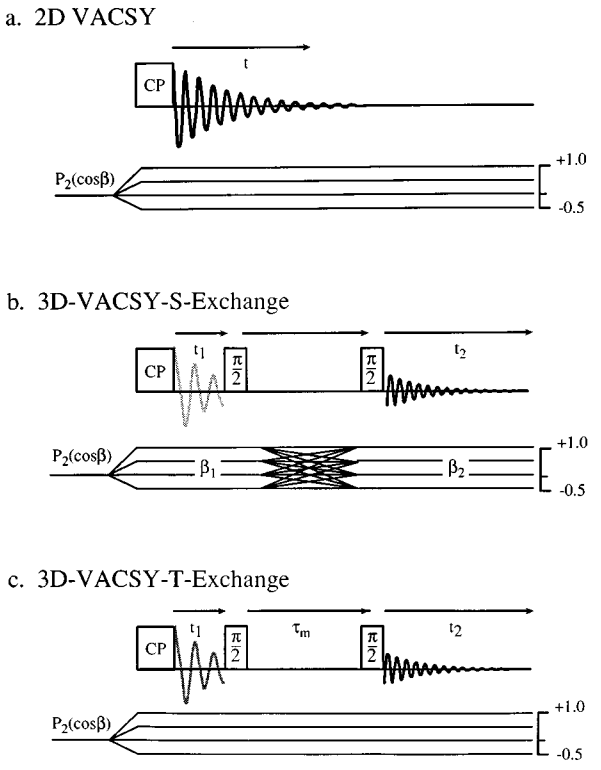

FIG. 1. Pulse sequences for carbon-13 VACSY experiments. For each sequence the carbon-13 rf pulses (above) and the corresponding tilt of the spinner axis, in terms of $P_2(\cos\beta)$ (below), are indicated. (a) 2D-VACSY used to correlate isotropic and anisotropic frequencies. Signals are acquired for different β's to form a 2D (t,β) data set. (b) 3D-VACSY-S-exchange used to record 2D correlation spectra for different isotropic frequencies. In this experiment t_1 is fixed while β_1, β_2, and t_2 are varied independently. Switching between the β's is done during the mixing time. (c) 3D-VACSY-T-exchange. In this version, t_1, β and t_2 are varied independently, but no switching of β is done during the pulse sequence.

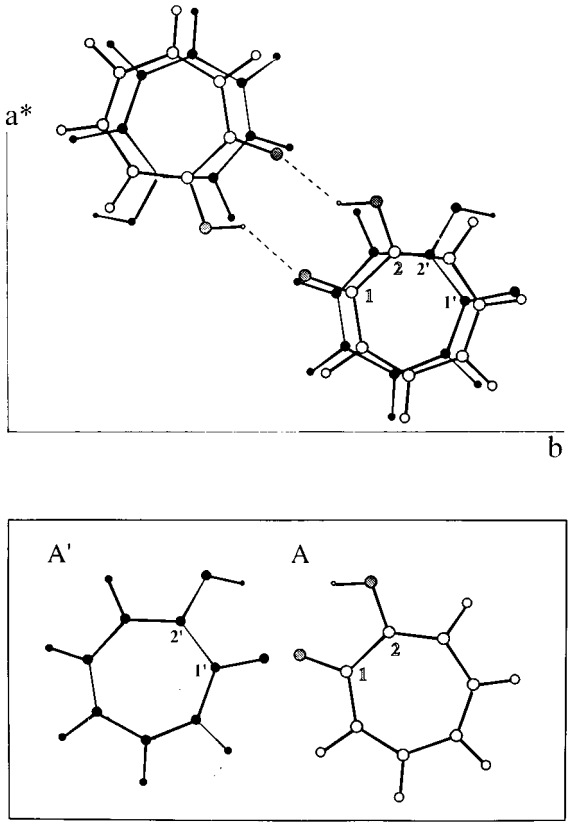

FIG. 2. *Top*: A projection of the crystal structure of tropolone onto the crystallographic **a***__b__ plane. The carbon sites, in the two crystallographic inequivalent (but symmetry related) molecules, are indicated by unprimed and primed numbers. *Bottom*: Projection of the two types of magnetically inequivalent tropolone molecules, relevant to the analysis of the NMR results.

exchange experiment,[7] and the procedure is repeated for different β values.

These experiments work well when the isotropic chemical shifts, ω_i, are not modulated by the spin exchange, so that for each ω_i a 2D exchange pattern can be obtained correlating the anisotropic interactions, ω_a, before and after the mixing time. If, however, the spin exchange involves different types of nuclei, the 3D-VACSY-exchange methods will not work, since they do not correlate between the different ω_t's. Such situations occur, for example, in solids exhibiting bond-shift rearrangements, as in bullvalene[8] and heptaphosphide trianions,[9] tautomeric hydrogen shift, such as certain NH and OH containing compounds,[10] or when the dominant process involves spin diffusion between different types of nuclei.[11–13] To include the effect of exchange in such systems, an extra time evolution period must be added to the 3D-VACSY-exchange experiments in order to introduce correlations between the isotropic chemical shifts. In the present work, we describe techniques that allow such experiments to be performed. However, in order to avoid the necessity of accumulating 4D data sets, we also propose simplified procedures, applicable in special simple cases, whereby the various correlations are obtained by a limited number of selective 2D-exchange experiments. These procedures make use of the SAS introduced over ten years ago by Terao and Maciel and their co-workers.[14,15] Subsequently, we apply such a method to study carbon-13 chemical shift correlations in tropolone.[16–18]

II. SELF-DIFFUSION AND SPIN DIFFUSION IN TROPOLONE

Tropolone crystallizes in the monoclinic space group $P2_1/c$ with two pairs of centrosymmetric hydrogen-bonded dimers per unit cell.[19] The molecules in the dimer are therefore magnetically equivalent, but the two dimers, although symmetry related, are not (see Fig. 2). It is, therefore, sufficient to consider just two NMR distinct molecules per unit cell. Earlier, carbon-13 MAS 2D exchange measurements by Szeverenyi *et al.*[16,17] showed the presence of a hydrogen shift process of the type

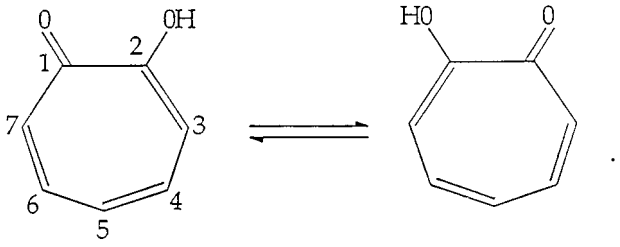

.

TABLE I. The four possible spin-exchange mechanisms in solid tropolone.

Mechanism		Correlation[a]		
Self-diffusion	Spin diffusion	1-1	2-2	1-2/2-1
1. Jump to a crystallographic equivalent site without molecular flip and without hydrogen shift.	Spin diffusion between magnetically equivalent nuclei.	⋯	⋯	⋯
2. Jump to a crystallographic equivalent site with both molecular flip and hydrogen shift.	Spin diffusion between different nuclei in crystallographic equivalent molecules.	⋯	⋯	$\lvert\gamma^1-\gamma^2\rvert$
3. Jump to a crystallographic inequivalent site with molecular flip, but without hydrogen shift.	Spin diffusion between the same type of nuclei in inequivalent molecules.	$2\gamma^1$	$2\gamma^2$	⋯
4. Jump to a crystallographic inequivalent site with hydrogen shift.	Spin diffusion between different nuclei in inequivalent molecules.	⋯	⋯	$\lvert\gamma^1+\gamma^2\rvert$

[a]The entries in this column correspond to the relative orientation between σ^k_{yy} and σ^l_{yy} of the chemical shift tensors of the correlated carbons.

The half-life of the reaction at 30 °C was found to be about 4 s with an activation energy of ~26 kcal/mol. The high-activation energy compared with that found for hydrogen shift in tropolone–cyclodextrin inclusion compounds[20] was ascribed to the molecular flip that must accompany the process in order to preserve the crystalline order in tropolone. A subsequent study[18] using rotor synchronized 2D exchange spectroscopy suggested that the dominant process, responsible for the dynamic features in the 2D-exchange spectra, is molecular self-diffusion, whereby the molecules jump between lattice sites in concert with planar reorientation and/or molecular flips. The hydrogen shift is a secondary reaction that follows whenever the jump diffusion results in swapping of the hydroxylic and carbonyl sites. Four types of jump diffusion mechanism have been distinguished,[18] depending on whether the jump is to a crystallographically equivalent or inequivalent site and whether or not it involves a hydrogen shift. The various mechanisms are summarized in Table I. Mechanism 1 is a translational jump to an equivalent site in the lattice that does not affect the NMR spectrum. Mechanism 2 is also a jump to an equivalent site, but involves a concerted molecular flip-hydrogen shift process. It corresponds to the original mechanism proposed by Szeverenyi *et al.*[17] Mechanisms 3 and 4 represent molecular jumps to inequivalent sites. However, while in mechanism 3 the molecules flip and no hydrogen shift is necessary, in mechanism 4 the molecules reorient in concert with a hydrogen shift. The various mechanisms affect the exchange correlation spectra in different ways. For example, mechanism 2 results in intramolecular pairwise exchange of carbons 1,2(1′,2′), 3,7(3′,7′) and 4,6(4′,6′), but leaves carbon 5(5′) unaffected; mechanism 3 results in spin exchange between similar carbons 1,1′, 2,2′, etc., while mechanism 4 corresponds to pairwise spin exchange of carbons 1,2′(1′,2), 3,7′(3′,7), 4,6′(4′,6), and 5,5′.

The original purpose of the present work was to determine separate rate constants for the various self-diffusion mechanisms. Carbon-13 VACSY-exchange methods seem ideal for that purpose, but in natural abundance the signals would be too weak to provide quantitatively interpretable results in reasonable measuring times. We have therefore prepared tropolone specifically enriched to 50% carbon-13 in position 1. Due to the tautomeric processes, the labeling is distributed between carbons 1 and 2 so that the sample actually contained 25% of singly labeled tropolone-1-^{13}C, 25% tropolone-2-^{13}C and 50% unlabeled tropolone. As discussed above, 2D correlation spectra of carbons 1 and 2 should allow us to distinguish between the various self-diffusion mechanisms.

Preliminary measurements on the enriched sample gave considerably faster values for the spin exchange rates compared with those reported by Szeverenyi *et al.*[17] for the isotopically normal compound. Similar observations were made by Olender *et al.*[20] when repeating the experiment of Titman *et al.*[18] in the enriched compound with a much weaker temperature dependence of the exchange rate. These observations suggest that while at natural carbon-13 abundance the magnetization transfer is indeed dominated by chemical exchange, at high isotopic enrichment it is mainly affected by spin diffusion. The effect of this mechanism on the magnetization transfer spectra is similar to that of the self-diffusion mechanisms, although the observed rates now depend on the dipolar interactions between the interchanging carbons[21,22] rather than the molecular self-diffusion. For both processes, however, at large mixing times the exchange spectra reflect the correlation between the chemical shift tensors of the interchanging sites. Since the crystal structure is known, these correlations provide information on the orientation of the chemical shift tensors in the molecular frame. In the present work, therefore, rather than determine the chemical exchange rates of the various self-diffusion mechanisms, we measured the various correlation spectra of the carbons 1 and 2 at large τ_m's in order to completely determine their chemical shift tensors. The approach follows that used by Robyr *et al.* and Tycko and Dabbagh in their determination of the carbon-13 chemical shift tensors in polycrystalline benzoic acid and methanol.[23,24]

In the Sec. III, methods for extending the 3D-VACSY-exchange experiments to nuclei with different isotropic chemical shifts are described. Such experiments necessitate

data acquisition in four dimensions and will probably be practical only in a few special cases. We therefore propose simplified procedures in which the desired correlations are obtained by a limited number of 2D experiments using SAS.[14,15] The synthetic procedure for preparing the labeled tropolone-1(2)-^{13}C, as well as details concerning the NMR measurements, are given in Sec. IV. The results are analyzed in Sec. V and briefly discussed in Sec. VI.

III. VACSY-EXCHANGE

A. The 3D-VACSY-exchange experiments

The 3D-pulse sequences shown in Figs. 1(b) and 1(c) extend the 2D-VACSY experiment [Fig. 1(a)] to the exchange regime.[5,6] These experiments are performed under conditions of fast spinning ($\omega_r > \omega_0 \delta\sigma$) with the spinning axis inclined at variable angles, β, to the external magnetic field. For an isolated nucleus, k, experiencing only chemical shift interactions, such as dilute carbon-13 under proton decoupling, the precession frequency of the magnetization in the rotating frame is

$$\omega^k(\vartheta,\phi) = \omega_i^k + \omega_a^k(\vartheta,\phi) P_2(\cos\beta), \tag{3.1}$$

where $P_2(\cos\beta)$ is the second order Legendre polynomial, ω_i^k is the isotropic frequency

$$\omega_i^k = \omega_0 \sigma_i^k, \tag{3.2}$$

and $\omega_a^k(\vartheta,\phi)$ is the anisotropic chemical shift interaction

$$\begin{aligned}\omega_a^k(\vartheta,\phi) = \omega_0[&\sigma_{11}^k \sin^2\vartheta \cos^2\phi + \sigma_{22}^k \sin^2\vartheta \sin^2\phi \\ &+ \sigma_{33}^k \cos^2\vartheta + \sigma_{12}^k \sin^2\vartheta \sin 2\phi \\ &+ \sigma_{13}^k \sin 2\vartheta \cos\phi + \sigma_{23}^k \sin 2\vartheta \sin\phi].\end{aligned} \tag{3.3}$$

Here ϑ and ϕ are the polar and azimuthal angles of the spinner axis, **z**, in the orthogonal axis system, **1,2,3**, of a particular crystallite, with ϑ the angle between **3** and **z** and ϕ being measured from **1**. The σ_{ij}^k $(i,j=1,2,3)$ are the components of the anisotropic chemical shift tensor of the k'th nucleus in the **1,2,3** coordinate system, such that

$$\sum_j \sigma_{jj}^k = 0 \tag{3.4}$$

and σ_i^k is the isotropic chemical shift. The total phase acquired by a particular spin during a 3D-VACSY-exchange experiment is

$$\begin{aligned}\Phi = &\omega_i^k t_1 + \omega_a^k(\vartheta,\phi) P_2(\cos\beta_1) t_1 + \omega_i^l t_2 \\ &+ \omega_a^l(\vartheta,\phi) P_2(\cos\beta_2) t_2,\end{aligned} \tag{3.5}$$

where k and l refer to the sites before and after the mixing period. For the case of enriched tropolone we need only consider $k,l = 1,1',2$ and $2'$. We distinguish between the following cases: (i) no spin exchange (including exchange between equivalent sites (mechanism 1 in Table I), $\omega_i^k = \omega_i^l$ and $\omega_a^k(\vartheta,\phi) = \omega_a^l(\vartheta,\phi)$; (ii) spin exchange between the same type of carbons (k,k') at different crystallographic sites (mechanism 3), $\omega_i^k = \omega_i^{k'}$ but $\omega_a^k(\vartheta,\phi) \neq \omega_a^{k'}(\vartheta,\phi)$; (iii) spin exchange between different types of atoms (mechanisms 2 and 4), $\omega_i^k \neq \omega_i^l$ and $\omega_a^k(\vartheta,\phi) \neq \omega_a^l(\vartheta,\phi)$.

In the 3D-VACSY-S-exchange experiment, t_1 is held fixed while β_1 and β_2 are varied independently, so that after redefining the variable time parameters, $(P_2(\cos\beta_1)t_1 = \tau_1$, $t_2 = \tau_2$, $P_2(\cos\beta_2)t_2 = \tau_3)$, Eq. (3.5) becomes

$$\Phi_S = \text{constant} + \omega_a^k(\vartheta,\phi)\tau_1 + \omega_i^l \tau_2 + \omega_a^l(\vartheta,\phi)\tau_3. \tag{3.6}$$

Three-dimensional Fourier transformation results in 2D correlations of the anisotropic interactions, $\omega_a^k(\vartheta,\phi)$ and $\omega_a^l(\vartheta,\phi)$, according to the isotropic chemical shifts ω_i^l during the detection period. For case (ii) this is equivalent to the usual 2D exchange (1), but when exchange also occurs between different carbons (case (iii)), the ω_i^l plane includes contributions due to spin exchange between the same type of carbons (l,l'), as well as from spin exchange between different types of carbons (k,l). Other choices of the independent time variables are, of course, possible, for example, two isotropic and one anisotropic time dimension.

The situation for 3D-VACSY-T-exchange is even more complicated. In this experiment t_1 is varied, but $\beta_1 = \beta_2$. After redefinition of the variables in Eq. (3.5) $(P_2(\cos\beta_1)t_1 = \tau_1$, $P_2(\cos\beta_2)t_2 = \tau_2)$ the total phase accumulated during the experiment becomes

$$\Phi_T = \omega_i^k t_1 + \omega_a^k(\vartheta,\phi)\tau_1 + \omega_i^l t_2 + \omega_a^l(\vartheta,\phi)\tau_2; \tag{3.7}$$

however, the four time variables t_1, τ_1, t_2, and τ_2 are, in general, not independent. For case (i), $\omega_i^k = \omega_i^l = \omega_i$, the first and third terms can be combined to $\omega_i^k t_1 + \omega_i^l t_2 = \omega_i \tau_3$ and the situation is similar to that for 3D-VACSY-S-exchange, but when exchange between different carbons occurs (case (iii)) it is not possible to define an independent τ_3.

B. The 4D-VACSY-exchange experiments

One way to correlate the ω_a's for different ω_i's is to augment the 3D-VACSY-exchange experiments with a fourth time-domain variable. This can be done by incrementing t_1 in the VACSY-S version, or equivalently, increment β_1 and β_2, independently, in the VACSY-T version. Equation (3.5) then becomes

$$\Phi = \omega_i^k \tau_1 + \omega_a^k(\vartheta,\phi)\tau_2 + \omega_i^l \tau_3 + \omega_a^l(\vartheta,\phi)\tau_4 \tag{3.8}$$

with all the τ_i's independent. The overall 4D time-domain signal obtained by suitable phase cycling is

$$\begin{aligned}I(\tau_1,\tau_2,\tau_3,\tau_4;\tau_m) = &\int_0^\pi d\vartheta \sin\vartheta \int_0^{2\pi} d\phi \sum_{k,l} P(k,l;\tau_m) \\ &\times \exp\{i[\omega_i^k \tau_1 + \omega_a^k(\vartheta,\phi)\tau_2 + \omega_i^l \tau_3 \\ &+ \omega_a^l(\vartheta,\phi)\tau_4]\},\end{aligned} \tag{3.9}$$

where $P(k,l;\tau_m)$ is the conditional probability that a nucleus initially at site k will be at site l a time τ_m later, and the summation is over all the discrete sites k,l. In writing Eq. (3.9) and in the following we neglect relaxation effects. Fourier transformation then yields a four-dimensional data set

$$S(\Omega_1,\Omega_2,\Omega_3,\Omega_4;\tau_m)$$
$$= \int d\tau_1 \int d\tau_2 \int d\tau_3 \int d\tau_4 I(\tau_1,\tau_2,\tau_3,\tau_4) \times \exp\{-i[\Omega_1\tau_1+\Omega_2\tau_2+\Omega_3\tau_3+\Omega_4\tau_4]\} \quad (3.10)$$

from which the various correlations can be projected out in the form of 2D exchange diagrams. For example, by setting $\Omega_1=\Omega_3=\omega_i^k$ a 2D correlation diagram is obtained corresponding to case (ii)

$$S(\Omega_1=\Omega_3=\omega_i^k,\Omega_2,\Omega_4;\tau_m)$$
$$= \sum_{k'} P(\omega^k,\omega^{k'};\tau_m) \int_0^{\pi} d\vartheta \sin\vartheta \int_0^{2\pi} d\phi \times \int d\tau_2 \int d\tau_4 \exp\{-i[\Omega_2-\omega_a^k(\vartheta,\phi)]\tau_2 - i[\Omega_4-\omega_a^{k'}(\vartheta,\phi)]\tau_4\}, \quad (3.11)$$

where the summation is over all sites having the isotropic chemical shift ω_i^k. If, on the other hand, we set $\Omega_1=\omega_i^k$, $\Omega_3=\omega_i^l\neq\omega_i^k$ the corresponding 2D correlation diagram will reflect spin exchange between sites having initially the isotropic frequency ω_i^k, but the frequency ω_i^l after the mixing time (case (iii))

$$S(\Omega_1=\omega_i^k,\Omega_3=\omega_1^l,\Omega_2,\Omega_4;\tau_m)$$
$$= \sum_{k',l'} P(\omega^{k'},\omega^{l'};\tau_m) \int_0^{\pi} d\vartheta \sin\vartheta \int_0^{2\pi} d\phi \int d\tau_2 \times \int d\tau_4 \exp\{-i[\Omega_2-\omega_a^{k'}(\vartheta,\phi)]\tau_2 - i[\Omega_4-\omega_a^{l'}(\vartheta,\phi)]\tau_4\}. \quad (3.12)$$

Note that this correlation spectrum is in general not symmetric with respect to the main diagonal, contrary to Eq. (3.11) (case (ii)) and the usual situation in 2D exchange spectroscopy. This is so because the $\Omega_1=\omega_i^k$, $\Omega_3=\omega_i^l\neq\omega_i^k$ plane selects only those nuclei that transform from sites k to sites l, but not those that undergo the reverse process. Microscopic reversibility requires that the reverse correlation spectrum, $S(\Omega_1=\omega_i^l,\Omega_3=\omega_i^k,\Omega_2,\Omega_4)$, be the mirror image of Eq. (3.12) about the main diagonal.

C. Selective switched-angle-spinning-2D-exchange experiments

Four-dimensional exchange experiments of the type described in the previous section are bound to be extremely time consuming. In certain situations one can simplify the experiment, by directly recording a small number of selected 2D correlation planes, instead of a full 4D exchange spectrum. This may be achieved using various modifications of SAS.[14,15] For example, by incorporating into a 2D exchange experiment two extra delays, before the evolution and before the detection periods, during which β is set to the magic angle and applying suitable pulse sequences that select the desired initial and final magnetizations. Several procedures for doing so have been used, including SELDOM,[25] DANTE,[26] and selective low-power rf pulses.[26] When the system contains just two types of spins, as is the case for the 1:1 mixture of tropolone-1-^{13}C and tropolone-2-^{13}C, the situation is particularly simple. One can prepare the spin system with only one site initially magnetized and likewise select one or the other magnetization for the detection. With this arrangement at most four 2D spectra need be recorded for the tropolone-1(2)-^{13}C case; actually only three of them are independent since, as indicated above, the ($\Omega_1=\omega_i^l$, $\Omega_3=\omega_i^k$) spectrum is related by symmetry to the ($\Omega_1=\omega_i^k$, $\Omega_3=\omega_i^l$) spectrum.

Figure 3(a) shows the basic pulse sequence used to monitor the various correlations involving carbons 1 and 2 in tropolone. By appropriate control of the rf frequency, the time delays, and the pulse phases, the 2D correlation diagrams, 1-1 ($\Omega_1=\Omega_3=\omega_i^1$), 1-2 ($\Omega_1=\omega_i^1$, $\Omega_3=\omega_i^2$), 2-1, and 2-2 were obtained. As an example, the sequence for the 2-1 correlation diagram was as follows: The tilt angle β was set to the magic angle and the spectrometer frequency adjusted to ω_i^2. Cross polarization, which created x-magnetization for both sites, was followed by a select sequence, consisting of a delay time $\tau_s=2\pi/(4\delta)$ (where $\delta=\omega_0|\sigma_i^1-\sigma_i^2|$) and a $\pi/2_y$ pulse which transformed the magnetization of site 2 to Zeeman order, leaving that of site 1 unaffected. The latter decayed to zero during the delay $\tau_h(T_2\ll\tau_h<T_1)$ which was also used to switch the angle β away from the magic angle, so as to optimize the effect of the anisotropic interaction during the evolution period. In our experiment, β was 79.4° ($P_2(\cos\beta)=-0.449$). A regular 2D-exchange experiment followed, but before the detection period a second select sequence was applied, this time retaining the magnetization of site 1. The final 2D data set, obtained by summation of properly phase-cycled subspectra, is

$$\sum_{2',1'} P(2',1';\tau_m) \exp\{i\omega_a^{2'}t_1+i[\omega_i^1+\omega_a^{1'}P_2(\cos\beta)]t_2\}, \quad (3.13)$$

where the summation is over each of the two sites of type 1 and 2. In practice, as the sequence in Fig. 3 shows, the FID following an echo, produced by a π-pulse at the first rotation echo, was recorded in order to minimize dead-time effects. Using similar procedures, the other correlation diagrams, 1-1, 2-2, and 1-2 were obtained. To minimize experimental artifacts, flip-flop of the cross polarization and Cyclops phase cycling were applied.

IV. EXPERIMENT

A. Preparation of tropolone-1-^{13}C

There are various ways to build up the seven-carbon ring skeleton of tropolone, but only a few of these reactions are useful for incorporating carbon-13 at the carbonyl position. Among those are the ring closure of suberonitrile with sodium methylanilide (Thorpe-Ziegler condensation)[27] and the decarboxylation of the calcium salt of suberic acid,[28] giving cycloheptanone in each case, followed by oxidation to cycloheptane-1.2-dione, bromination, and finally dehydrobromination to tropolone. The more classical ''organic syn-

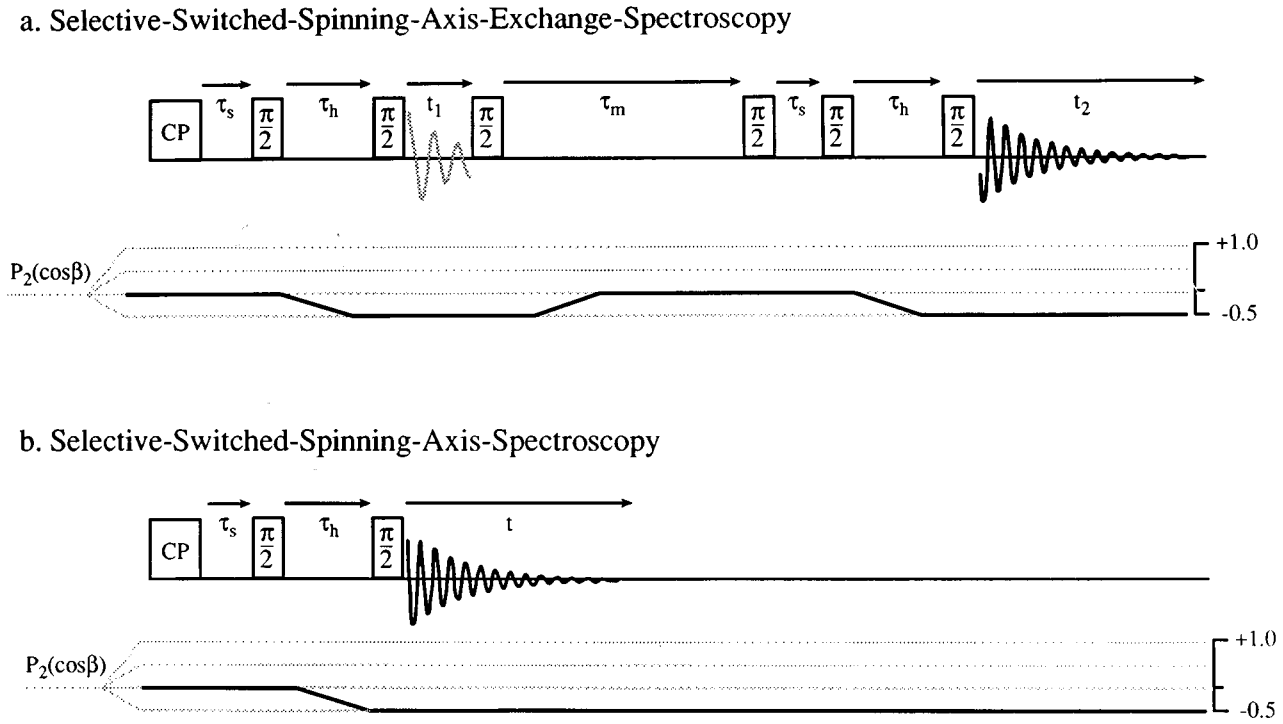

FIG. 3. (a) The pulse sequence used to obtain selective 2D correlation spectra. (b) Pulse sequence used for selective recording of powder spectra.

thesis'' procedure proceeds via 7.7-dichlorobicyclo (3.2.0) hept-2-en-6-one[29] followed by hydrolysis to tropolone.[30] In order to label tropolone in the 1 position with *C*-13 we selected the last reaction. This requires the synthesis of dichloroacetylchloride-1-^{13}C in order to generate carbonyl-labeled dichloroketene, which is reacted with cyclopentadiene to yield the final product, as shown in the following reaction scheme:

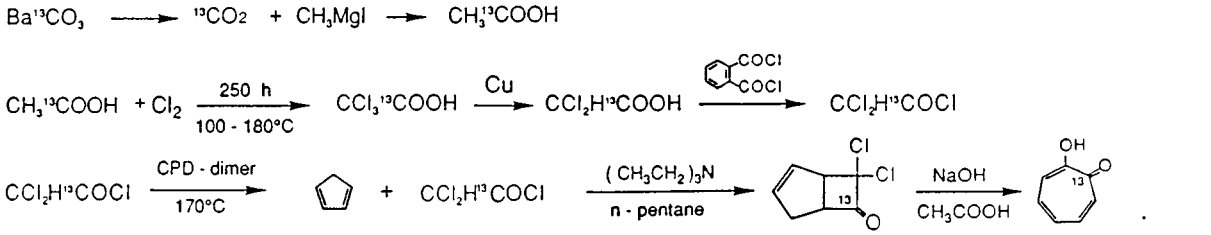

Acetic acid-1-^{13}C was prepared by carboxylation of methylmagnesiumiodide with $^{13}CO_2$. A sample of 50% enriched acid was chlorinated with Cl_2 to give trichloroacetic acid-1-^{13}C, followed by dechlorination[31] with copper to dichloroaceticacid-1-^{13}C and reaction with *o*-phthaloylchloride to dichloroacetylchloride. Reaction of the latter compound with triethylamine produced carbonyl-C-13-labeled dichloroketene *in situ*[29,30] which underwent cycloaddition with cyclopentadiene (CPN) to give 7.7-dichlorobicyclo(3.2.0)-hept-2-en-6-one-6-^{13}C. Hydrolysis of this adduct yields tropolone-1-^{13}C. Application of this reaction pathway allows the use of barium carbonate-^{13}C as the isotopic source, and results in a precise and economic incorporation of carbon-13 at position 1 of the tropolone molecule. Tautomerism then distributes the ^{13}C nuclei equally between sites 1 and 2, with only singly labeled molecules.

Trichloroacetic acid-1-^{13}C: 15 g acetic acid-1-^{13}C (50% carbon-13) was gradually chlorinated with elemental chlorine gas; the reaction temperature was raised from 105 to 190 °C over 180 h. Care was taken to ensure that the loss due to evaporation was kept to a minimum. The chlorination was monitored by ^{1}H- and ^{13}C-NMR until no proton resonances from the methyl group were observed. After bulb-tube distillation under reduced pressure, 23 g of trichloroacetic acid-1-^{13}C was obtained.

Dichloroacetic acid-1-^{13}C: 23 g of the labeled trichloro-

acetic acid was dissolved in 190 ml of water in a reaction flask with a mechanical stirrer. 11.7 g of copper bronze was then added while the temperature was raised to 60 °C. The reaction is quite exothermic and heating was discontinued after this temperature was attained. After stirring for 90 min, the mixture was refluxed for 1 h during which time the color changed from green to white (due to the precipitation of cuprous chloride). After cooling, the salt was filtered off and washed with a small amount of water. The filtrate was saturated with hydrogen sulfide until the precipitation of copper sulfides was complete. After filtration the slightly yellow filtrate was concentrated under reduced pressure, and the residue was fractionated at 20 mm pressure, yielding 13.2 g of dichloroacetic acid-1-^{13}C, b.p.=102 °C, contaminated (according to NMR) with approximately 4%–5% of monochloroacetic acid.

Dichloroacetylchloride-1-^{13}C: 33 ml of *o*-phthaloylchloride was heated to 140 °C, and 13.2 g of the labeled dichloroacetic acid added dropwise. The mixture was kept at this temperature for 1 h and then distilled at atmospheric pressure using a small Vigreux distillation column until the oil bath reached 180 °C. 10.3 g of dichloroacetylchloride-1-^{13}C was isolated, b.p.=107–109 °C.

7.7-*dichlorobicyclo* (3.2.0)-hept-2-en-6-one-6-^{13}C: 10 g dichloroacetylchloride-1-^{13}C and 8.95 g cyclopentadiene [freshly prepared from dicyclopentadiene (Aldrich) by distillation] were mixed together in 60 ml dry *n*-hexane. 9.5 ml triethylamine (dried over KOH pellets) was added dropwise over 2 h at room temperature with efficient stirring and continuous nitrogen bubbling. The mixture was stirred overnight, and then filtered through a *G*-2 glass filter, and the salt was washed with dry *n*-hexane. The solvent was removed at 100 Torr, and the red-brown residue was distilled under high vacuum, resulting in 8.2 g of a clear distillate, 7.7-dichlorobicyclo (3.2.0)-hept-2-en-6-one-6-^{13}C, b.p.=49 °C at 0.3 Torr. The site of the labeling was confirmed by the carbonyl signal (at 197.7 ppm) in the carbon-13 NMR spectrum of a $CDCl_3$ solution of the compound.

Tropolone-1-^{13}C: 8 g NaOH pellets were added to 40 ml glacial acetic acid, and the mixture was stirred and heated until a clear solution was obtained. 8 g of the labeled cycloadduct was added and the solution was refluxed overnight with slow nitrogen bubbling. The mixture was cooled, acidified to *p*H 1 with conc. HCl, and 100 ml benzene was added. After filtration the precipitate was washed with additional benzene, and the filtrate was separated into aqueous and organic phases. The aqueous phase was subjected to a 10 h liquid–liquid extraction with benzene and the extract combined with the original benzene phase. The extract was concentrated under vacuum, and the red residue was fractionally distilled under high vacuum yielding 5.8 g of a slightly yellow solid. This was redistilled in a bulb tube and finally sublimed twice under reduced pressure resulting in 4.1 g tropolone-1-^{13}C as a white crystalline solid, m.p.=52–53 °C, with $m/z=122$, 123 of equal intensity. Carbon-13 NMR (in a $CDCl_3$ solution) exhibits a strong peak at 171.8 ppm due to carbons 1,2 of tropolone and well-resolved satellites of the natural abundance 3,7 carbons (at 128.2 ppm, with $J\sim135$ Hz), thus confirming the labeling site as the oxygen-bound carbons 1 and 2.

B. NMR measurements

Carbon-13 NMR spectra were recorded at 75.45 MHz using a home-built spectrometer equipped with a room-temperature hopping-coil probe.[32] The spinner outer diameter was 7 mm and it contained ~370 mg tropolone. The spinning rate was ~6.5 kHz. Due to arcing problems relatively low rf power was used, corresponding to $\pi/2$ pulse widths of 4–10 μs. Different pulse widths were applied for different spinning angles, to account for the $\sin\beta$ dependence of the transverse rf field. The estimated hopping time of the rf coil is 30 ms, much shorter than the designated hopping delays in the pulse sequence. The recycle time was 45 s. Usually 64 points were acquired during acquisition and 30–40 points in the t_1-dimension. The dwell time was 67 μs in each dimension, corresponding to an overall spectral width of 15 kHz ($\pm$7.5 kHz). The whole data set was apodized with a 200 Hz Gaussian line broadening function in each dimension and zero filled to a 128×128 data square before Fourier transformation.

V. RESULTS AND ANALYSIS

A. The chemical shift tensors

To determine the principal values of the chemical shift tensors of carbons 1 and 2 in the enriched tropolone sample we used a selective SAS experiment similar to that described in Refs. 25, 26, and 33. The pulse sequence used is shown in Fig. 3(b). With the spinner axis inclined at the magic angle and the spectrometer frequency set at resonance with one of the carbons, either of the two magnetizations can be selected as described above for the SAS experiments. During the second delay, τ_h, the spinning axis is switched off the magic angle (to $\beta=79.4°$) and the signal following an echo π-pulse, applied at the first rotation echo (not shown), is recorded. The resulting signal, expressed in terms of the principal values of the chemical shift tensor of the selected nucleus, k, is

$$I(t)\sim \exp\{i[\omega_i^k+\omega_a^k(\vartheta,\phi)P_2(\cos\beta)]t\}, \tag{5.1}$$

where ϑ and ϕ are now the polar and azimuthal angles of the spinner axis in the principal coordinate system **x**,**y**,**z**, of the chemical shift tensor and

$$\omega_a^k(\vartheta,\phi)=\frac{\omega_0\delta\sigma^k}{3}(3\cos^2\vartheta-1+\eta^k\sin^2\vartheta\cos 2\phi), \tag{5.2a}$$

with

$$\delta\sigma^k=\sigma_{zz}^k-\frac{1}{2}(\sigma_{xx}^k+\sigma_{yy}^k),$$
$$\eta^k=\frac{\sigma_{xx}^k-\sigma_{yy}^k}{\sigma_{zz}^k}, \tag{5.2b}$$
$$\sigma_{xx}^k+\sigma_{yy}^k+\sigma_{zz}^k=0$$

and we have chosen $\sigma_{xx}^k>\sigma_{yy}^k>\sigma_{zz}^k$. The overall signal is the integral of Eq. (5.1) over ϑ and ϕ. Fourier transformation

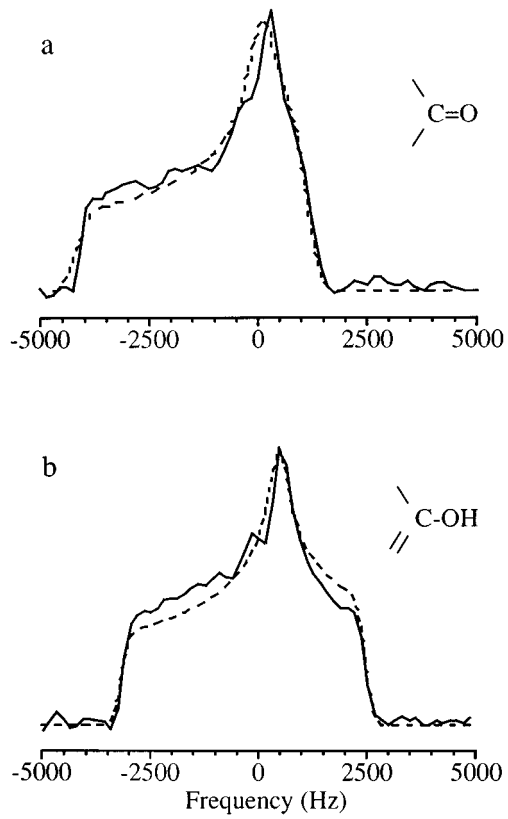

FIG. 4. Experimental (full line) $P_2(\cos\beta)$-scaled powder spectra for carbons 1 (a) and 2 (b) of tropolone obtained by sequence (b) of Fig. 3, for $\beta=79.4°$ ($P_2(\cos\beta)=-0.449$) and using a Gaussian line broadening of 200 Hz. The dashed line is calculated using the SAS chemical shift parameters of Table II. The zero frequency corresponds to the isotropic chemical shift of carbon 2, $\omega_i^2=0$.

results in a usual powder pattern, but scaled according to $P_2(\cos\beta)$. Results so obtained for carbons 1 and 2 in the enriched tropolone sample are shown in Fig. 4, yielding the chemical shift tensors as summarized in Table II. For comparison we also show the results of an earlier study[18] based on the analysis of spinning sideband intensities[34] in MAS spectra.

These results do not provide information on the orientation of the principal components of the chemical shift tensors in the molecular frame, although partial assignment can be made on the basis of some generally known properties of such tensors for carbon-13 nuclei.[35,36] For example, it is safe to assume that the direction of the most shielded tensor component, σ_{zz}, is perpendicular to the molecular plane while the intermediate component is expected to lie close to the double bond associated with the particular carbon. In general, the determination of the exact orientation of the chemical shift tensor requires measurements on single crystals, which were, however, not available to us for tropolone. Instead, we use spin-diffusion correlation spectroscopy[23,24] to determine the relative orientations of the carbons 1 and 2 chemical shift tensors and from the known crystal structure[19] also their absolute orientation in the molecular frame.

To simplify the analysis, we shall assume that the tropolone molecules lie in the **a*****b**-plane, neglecting a small tilt (5°) between the perpendicular to the molecular plane and **c**. We also assume that the σ_{zz}'s of both carbons 1 and 2 lie perpendicular to the molecular plane, so that the only remaining parameters are the orientations of the σ_{yy}'s in the **a*****b**-plane. Identifying the crystallographic **a***,**b**,**c** axis with the crystal fixed orthogonal system **1,2,3** Eq. (3.3) the chemical-shift components in this frame become

$$\sigma_{33}^k=\sigma_{zz}^k, \tag{5.3a}$$

$$\sigma_{11}^k=\sigma_{xx}^k\sin^2\gamma^k+\sigma_{yy}^k\cos^2\gamma^k, \tag{5.3b}$$

$$\sigma_{22}^k=\sigma_{xx}^k\cos^2\gamma^k+\sigma_{yy}^k\sin^2\gamma^k, \tag{5.3c}$$

$$\sigma_{12}^k=\tfrac{1}{2}(\sigma_{yy}^k+\sigma_{xx}^k)\sin^2\gamma^k, \tag{5.3d}$$

$$\sigma_{13}^k=\sigma_{23}^k=0, \tag{5.3e}$$

where γ^k is the angle between σ_{yy}^k and the **b**(**2**) axis. Since the two magnetically inequivalent molecules in the crystal are related by a glide reflection plane parallel to **a*****c** (**13**), we have $\gamma^1=-\gamma^{1'}$ and $\gamma^2=-\gamma^{2'}$.

B. Spin diffusion correlation experiments

The correlation time, τ_c, for the spin exchange in our enriched sample at room temperature is about 1 s. To obtain 2D correlation spectra between the various tensors of carbons 1 and 2 Eq. (3.13) two sets of selective switched spinning angle 2D-exchange experiments were performed with mixing times, τ_m, much shorter (0.1 s) and much longer (6.0 s) than the estimated τ_c. For the short mixing time we have $P(k,l;\tau_m\to 0)\sim\delta_{k,l}$, while for the long mixing time, $P(k,l;\tau_m\to\infty)\sim P(l)=\frac{1}{4}$, the equilibrium distribution of site l. For each mixing time, four selective 2D-exchange spectra were recorded, 1-1, 2-2, 1-2, and 2-1, where the indices k-1 refer to the initial and final isotropic frequencies, ω_i^k and ω_i^l.

TABLE II. The chemical shift-shielding tensor components of carbons 1 and 2 of tropolone.[a,b]

	Carbon 1					Carbon 2				
	σ_{xx}	σ_{yy}	σ_{zz}	σ_i	$2\gamma^e$	σ_{xx}	σ_{yy}	σ_{zz}	σ_i	$2\gamma^e$
SAS[c]	65	33	−98	178.1	56°	77	17	−94	166.2	28°
MAS[d]	65	25	−90	178.1	⋯	75	15	−90	166.2	⋯

[a]$\sigma_{xx}+\sigma_{yy}+\sigma_{zz}=0$.
[b]σ_i is relative to TMS, taken from Ref. 16.
[c]From present work. Estimated error ± ppm.
[d]From Ref. 16. There is a misprint in the value of σ_{yy}^2 in the original paper.
[e]$2\gamma^k$ is the angle between the directions of σ_{yy}^k and $\sigma_{yy}^{k'}$, for $k=1$ and 2.

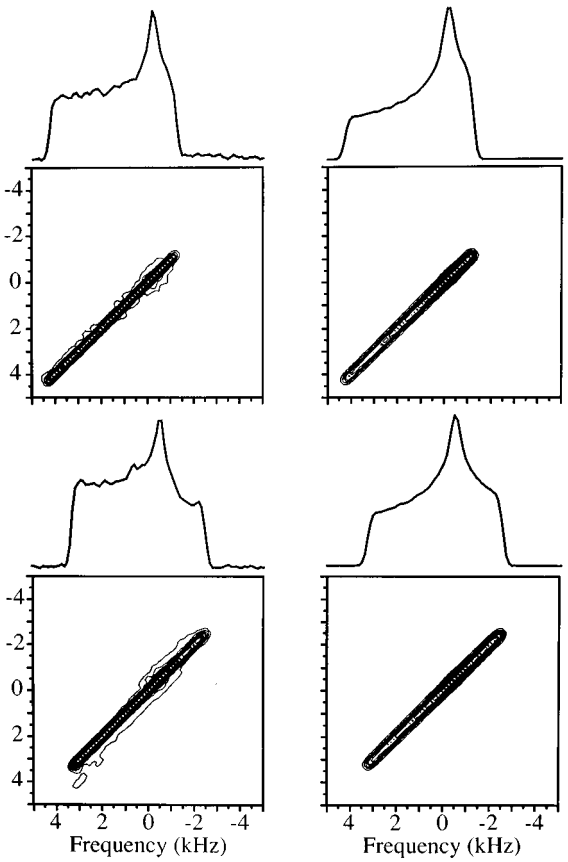

FIG. 5. *Left*: Experimental 2D correlation spectra of carbons 1 (top) and 2 (bottom) of tropolone, obtained by pulse sequence (a) of Fig. 3, with $\tau_m=0.1$ s($\ll\tau_c$) and a Gaussian line broadening of 200 Hz. *Right*: Simulated static 2D spectra ($\tau_m=0$) obtained with the chemical shift parameters of Table II. Also shown are skyline projections for each case. In all spectra there are 20 equally spaced contours between 5% and 100% of maximum intensity.

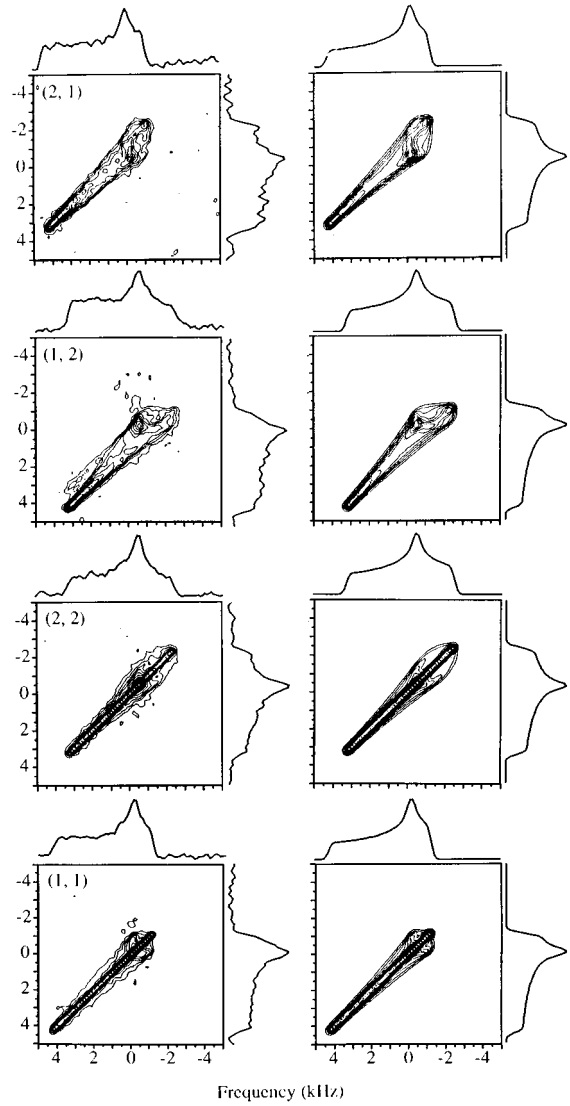

FIG. 6. Experimental (left) and calculated (right) 2D correlation spectra for the carbon sites 1-1, 2-2, 1-2 and 2-1 for $\tau_m=6.0$ s($\gg\tau_c$). The parameters used in the simulations are given in Table II. The Gaussian line broadening and contour spacings are as in Fig. 5, except that for the 1-2 and 2-1 spectra there are 11 equally spaced contours between 9% and 100% of the maximum intensity.

On the left side of Fig. 5 are shown experimental results for the 1-1 and 2-2 planes for $\tau_m=0.1$ s. Only single ridges along the main diagonal are observed as expected for the case of no spin exchange. These ridges are the projections of the $P_2(\cos\beta)$-scaled powder spectra of carbons 1 and 2 and can well be simulated with the chemical shift parameters of Table II, as shown on the right side of Fig. 5. No signals were observed in the 1-2 and 2-1 correlation experiments in the $\tau_m=0.1$ s experiments.

On the left side of Fig. 6 are shown selective 2D exchange spectra for a mixing time of 6.0 s. The situation is now quite different. There is considerable intensity outside the main diagonal in the 1-1 and 2-2 correlation spectra and there are well-defined contours also in the 1-2 and 2-1 spectra. The 1-1 and 2-2 correlation spectra are due to spin exchange between carbons 1,1′ and carbons 2,2′ (mechanism 4 of Table I). Since $\tau_m\gg\tau_c$, each 2D spectrum consists of a 1:1 superposition of subspectra due to carbon spins that at the end of the mixing time retained their original site and those that switched sites. To determine the γ^k's we compared the experimental results with calculated 2D correlation spectra for different γ^k values. Such calculated spectra for the two carbons are shown in Fig. 7. By visual comparison with the experimental results, the following best-fit values for γ^k were obtained, $2\gamma^1=56°$ and $2\gamma^2=28°$. The corresponding spectra are reproduced on the right side of Fig. 6. [Because of the forms of Eq. (5.3) it is not possible to distinguish between γ^k and $(\pi/2)-\gamma^k$. We give the smaller values of the two alternatives.] These results are quite reasonable: $2\gamma^k$ corresponds to the angle between σ^k_{yy} and $\sigma^{k'}_{yy}$ for both $k=1$ and 2. From the crystal structure we know that the angle between the $C^1=O^1$ and $C^{1'}=O^{1'}$ bonds is 32°. Comparison with $2\gamma^1=56°$ shows that σ^1_{yy} lies 12° off the C=O bond direction towards the hydroxyl carbon. Similarly, the angle between $C^3=C^2$ and $C^{3'}=C^{2'}$ is 7°, so that σ^2_{yy} lies 10° off the $C^3=C^2$ bond, away from the carbonyl group.

In the 2-1 and 1-2 correlation spectra there are only off-diagonal intensities [except for contributions due to special orientations for which $\omega^k_a(\vartheta,\phi)=\omega^l(\vartheta,\phi)$] and, as ex-

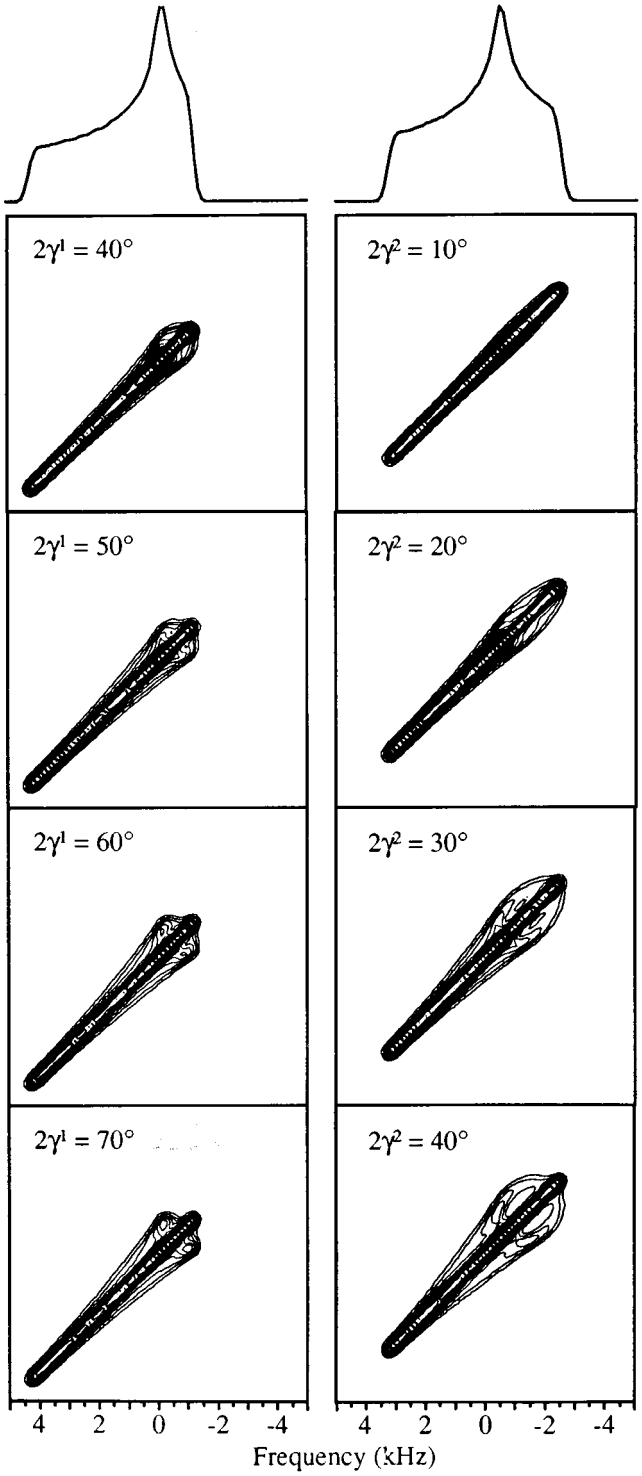

FIG. 7. Simulation of the 1-1 (left) and 2-2 (right) correlation spectra of tropolone for different $2\gamma^k$ values. Each spectrum is a 1:1 superposition of spectra due to $2\gamma^k=0°$ and the indicated $2\gamma^k$ value. The chemical shift parameters are from Table II, and the Gaussian line broadening and contour levels are as in Fig. 5.

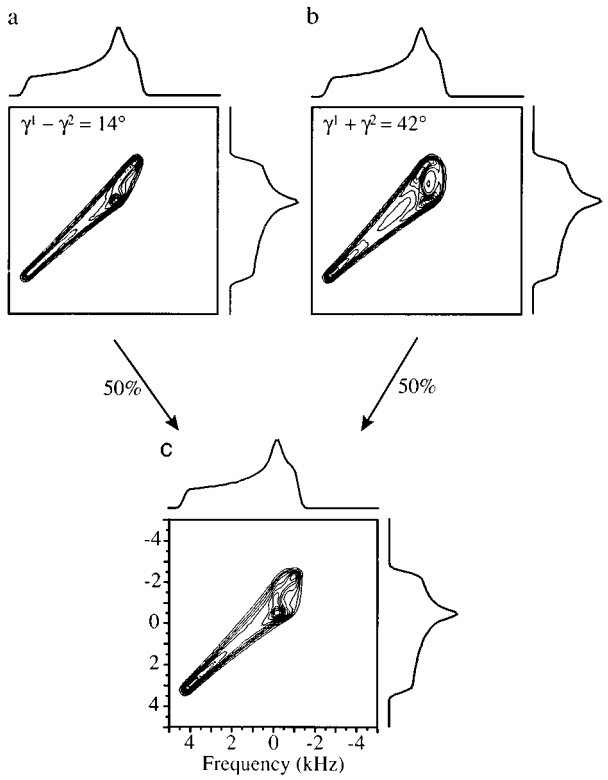

FIG. 8. Simulated correlation spectra for (a) mechanism 2 with $\gamma^1-\gamma^2=14°$ and (b) mechanism 4 with $\gamma^1+\gamma^2=42°$. (c) A 1:1 superposition of spectra a and b. Gaussian line broadening and contour levels as in Fig. 5.

pected, the two spectra are mirror images of each other. It is therefore sufficient to consider just one of the two. Two mechanisms contribute to the 1-2 correlation spectrum, i.e., spin exchange between carbons 1 and 2 (also 1′ and 2′) and spin exchange between carbons 1 and 2′ (1′ and 2), corresponding to effective reorientation angles of $|\gamma^1-\gamma^2|$ and $|\gamma^1+\gamma^2|$, respectively (mechanisms 2 and 4 in Table I). Since γ^1 and γ^2 are fixed by the previous experiments, there are no free parameters left to fit these results. In Fig. 8 are shown simulated 1-2 correlation diagrams for the two mechanisms as well as their 1:1 superpositions. The two correlation spectra are quite distinct from each other and exhibit characteristic features which do not fit the experimental result. On the other hand, their 1:1 superposition agrees satisfactorily with the 1-2 correlation spectrum in Fig. 6. This shows that the correlation time for all mechanisms is much shorter than the mixing time (6 s) used in these experiments.

VI. SUMMARY AND CONCLUSIONS

The main results of the present study concern the determination of carbon-13 chemical shift tensor in a polycrystalline sample of tropolone, using 2D correlation spectroscopy. In principle, single-crystal studies should be more accurate. However, such samples are not always available and if they are they require accurate crystal mounting and may be quite time consuming. Two-dimensional correlation spectroscopy uses internal referencing and its accuracy depends essentially only on the quality of the experimental results. Both methods may suffer from ambiguities in signal identification when the system contains symmetry related sites as in tropolone. We have circumvented the problem by associating the σ_{yy}'s with the nearest double bond, but in principle the assignment

could be inverted. Comparison with theoretical predictions could be very helpful in eliminating such ambiguities.

The 2D-exchange SAS method used in this work is similar to the rotor synchronized MAS 2D exchange method.[2,3] Both provide correlations between chemical-shift tensors coupled by spin-exchange mechanisms. The latter method may be superior signal-to-noise wise since the whole spectrum intensity is concentrated in a limited number of spinning sidebands, while the contour patterns of the former method often provide a more direct indication on the nature of the correlations.

ACKNOWLEDGMENTS

This work was supported by the U.S.–Israel Binational Science Foundation, Jerusalem and by the MINERVA Foundation, Munich/Jerusalem, and by the Director, Office of Energy Research, Office of Basic Energy Sciences, Materials Sciences Division of the U.S. Department of Energy under Contract No. DE-AC03-76SF00098.

[1] H. W. Spiess, Chem. Rev. **1**, 1321 (1991); B. H. Meier, Adv. Magn. Opt. Reson. **18**, 1 (1994); K. Schmidt-Rohr and H. W. Spiess, *Multidimensional Solid-State NMR and Polymers* (Academic, London, 1994).
[2] A. F. de Jong, A. P. M. Kentgens, and W. S. Weeman, Chem. Phys. Lett. **109**, 337 (1984).
[3] A. Hagemeyer, K. Schmidt-Rohr, and H. W. Spiess, Adv. Magn. Reson. **80**, 401 (1988).
[4] L. Frydman, G. C. Chingas, Y. K. Lee, P. J. Grandinetti, M. A. Eastman, G. A. Barrall, and A. Pines, J. Chem. Phys. **97**, 4800 (1992).
[5] L. Frydman, Y. K. Lee, L. Emsley, G. C. Chingas, and A. Pines, J. Am. Chem. Soc. **115**, 4825 (1993).
[6] Y. K. Lee, L. Emsley, R. G. Larsen, K. Schmidt-Rohr, M. Hong, L. Frydman, G. C. Chingas, and A. Pines, J. Chem. Phys. **101**, 1852 (1994).
[7] J. Jeener, B. H. Meier, P. Bachmann, and R. R. Ernst, J. Chem. Phys. **71**, 4546 (1979).
[8] B. H. Meier and W. L. Earl, J. Am. Chem. Soc. **107**, 5553 (1985).
[9] M. Baudler and K. Glinka, Chem. Rev. **93**, 1623 (1993).
[10] H.-H. Limbach, *NMR Basic Principles and Progress* (Springer-Verlag, Berlin, 1990), Vol. 23, p. 63.
[11] N. M. Szeverenyi, M. J. Sullivan, and G. M. Maciel, J. Magn. Reson. **47**, 462 (1982); C. E. Bronniman, N. M. Szeverenyi, and G. M. Maciel, J. Chem. Phys. **79**, 3694 (1983).
[12] M. Linder, M. Henrichs, J. M. Hewitt, and D. J. Massa, J. Chem. Phys. **82**, 1585 (1985).
[13] D. L. Vanderhart, J. Magn. Reson. **72**, 13 (1987).
[14] A. Bax, N. M. Szeverenyi, and G. E. Maciel, J. Magn. Reson. **15**, 494 (1983).
[15] T. Terao, T. Fujii, T. Onodera, and A. Saika, Chem. Phys. Lett. **107**, 145 (1984).
[16] N. M. Szeverenyi, M. J. Sullivan, and G. E. Maciel, J. Magn. Reson. **47**, 462 (1982).
[17] N. M. Szeverenyi, A. Bax, and G. E. Maciel, J. Am. Chem. Soc. **105**, 2579 (1983).
[18] J. J. Titman, Z. Luz, and H. W. Spiess, J. Am. Chem. Soc. **114**, 3756 (1992).
[19] H. Shimanuchi and Y. Sasada, Acta Crystallogr. B **29**, 81 (1973).
[20] Z. Olender, D. Reichert, A. Müller, H. Zimmermann, R. Poupko, and Z. Luz (unpublished).
[21] R. Eckman, A. Pines, R. Tycko, and D. P. Weitekamp, Chem. Phys. Lett. **99**, 35 (1983).
[22] D. Suter and R. R. Ernst, Phys. Rev. B **32**, 5608 (1985).
[23] P. Robyr, B. H. Meier, and R. R. Ernst, Chem. Phys. Lett. **187**, 471 (1991); P. Robyr, B. H. Meier, P. Fischer, and R. R. Ernst, J. Am. Chem. Soc. **116**, 5315 (1994).
[24] R. Tycko and G. Dabbagh, J. Am. Chem. Soc. **113**, 3592 (1991); Isr. J. Chem. **32**, 179 (1992).
[25] P. Tekely, J. Brondeau, K. Elbayed, A. Retournard, and D. Canet, J. Magn. Reson. **80**, 509 (1988).
[26] J. H. Iwamiya, M. F. Davis, and G. E. Maciel, J. Magn. Reson. **88**, 199 (1990).
[27] K. Ziegler, H. Eberle, and H. Ohlinger, Justus Liebigs Ann. Chem. **504**, 120 (1933); K. Ziegler and R. Aurnhammer, *ibid*. **513**, 57 (1934).
[28] J. N. E. Day, G. A. R. Kon, and A. Stevenson, J. Chem. Soc. 642 (1920); T. Nozoe, Y. Kitahara, T. Ando, and S. Masamune, Proc. Jpn. Acad. **27**, 415 (1951).
[29] P. A. Grieco, J. Org. Chem. **37**, 2363 (1972).
[30] R. A. Minns, Org. Synth. **57**, 118 (1977).
[31] H. W. Doughty and G. J. Derge, J. Am. Chem. Soc. **53**, 1595 (1931).
[32] M. A. Eastman, P. J. Grandinetti, Y. K. Lee, and A. Pines, J. Magn. Reson. **98**, 333 (1992).
[33] J. Ashida, T. Nakai, and T. Terao, Chem. Phys. Lett. **168**, 523 (1990).
[34] J. Herzfeld and A. E. Berger, J. Chem. Phys. **73**, 6021 (1980).
[35] W. S. Veeman, Proc. Nucl. Magn. Reson. Spectrosc. **16**, 193 (1984).
[36] M. H. Sherwood, J. C. Facelli, D. W. Alderman, and D. M. Grant, J. Am. Chem. Soc. **113**, 750 (1991).